EXPERIMENTAL AND NUMERICAL INVERSTIGATION ON CROSS FLOW IN THE PMR200 CORE

J.H. Lee, S.J. Yoon, D.H. Shin, H.K. Cho*, G.C. Park
*Author for correspondence
Department of Nuclear Engineering,
Seoul National University,
Seoul, 151-744,
Korea,
E-mail: chohk@snu.ac.kr

ABSTRACT

The Prismatic Modular Reactor (PMR) is one of the major Very High Temperature Reactor (VHTR) concepts, which consists of hexagonal prismatic fuel blocks and reflector blocks made of nuclear grade graphite. However, the shape of graphite blocks could be easily changed by neutron damage during the reactor operation and the shape change can make the gaps between the blocks inducing bypass flow. Two types of gap shape should be considered. The vertical gap and horizontal gap are called bypass gap and cross gap, respectively. The cross gap complicates flow field in reactor core by connecting coolant channel and bypass gap and it could lead to loss of effective coolant flow in fuel blocks. In this paper, cross flow experimental facility was constructed to investigate the cross flow phenomena in the core of the VHTR and the experiment was carried out under varying flow rates and gap sizes. The results of the experiments were compared with CFD (Computational Fluid Dynamics) analysis results. In order to apply the CFD code to the cross flow phenomena, the prediction capability of the CFD code was verified. Good agreement between experimental results and CFD predictions was observed and the characteristics of the cross flow was discussed in detail.

INTRODUCTION

Very High Temperature Reactor (VHTR), one of the Generation-IV (Gen-IV) reactors, is uranium-fueled, graphite-moderated and helium-cooled reactor. It has several advantages over the previous generation reactor; these include enhanced fuel integrity, proliferation resistance, relatively simple fuel cycle and modularity to supply electricity [1]. Prismatic modular reactor (PMR) is one of the prospective VHTR core type candidates. PMR200 is considered as a candidate for the Nuclear Hydrogen Development and Demonstration plant [2]. The core of the PMR type reactor consists of assemblies of hexagonal graphite blocks. The graphite blocks have lots of advantages for neutron economy and high temperature structural integrity [3]. The height and flat-to-flat width of fuel bock are 793 mm and 360 mm, respectively. Each block has 108 coolant channels of which the diameter is 16 mm. And there are gaps between blocks not only vertically but also horizontally for reloading of the fuel elements. The vertical gap induces the bypass flow and through the horizontal gap the cross flow is formed. Since the complicated flow distribution occurs by the bypass flow and cross flow, flow characteristics in the core of the PMR reactor cannot be treated as a simple pipe flow.

The fuel zone of the PMR core consists of multiple layers of fuel blocks. The shape change of the fuel blocks could be caused by the thermal expansion and fast-neutron induced shrinkage. It could make different axial shrinkage of fuel block and this leads to wedge-shaped gaps between two stacked fuel blocks. The cross flow is often considered as a leakage flow through the horizontal gap between stacked fuel blocks and it complicates the flow distribution in the reactor core by connecting the coolant channel and the bypass gap. Moreover, the cross flow could lead to uneven coolant distribution and consequently cause superheating of individual fuel element zones with increased fission product release. Since the core cross flow has a negative impact on safety and efficiency of VHTR, core cross flow phenomena have to be investigated to improve the core thermal margin of VHTR [4]. For this reason, studies on cross flow were conducted by Groehn (1982) in German [5] and Kaburaki (1990) in Japan [6]. However, the shape of fuel blocks in previous study differs from that of NHDD PMR-200 fuel block and the cross flow loss coefficient for PMR-200 core has not been studied sufficiently. To develop the cross flow loss coefficient model to determine the flow distribution for PMR core analysis codes, study on cross flow for PMR-200 core is essential. In particular, to predict the amount of flow through the cross flow gap, obtaining accurate flow loss coefficient is important.

In this study, the full-scale cross flow experimental facility was constructed to represent the cross flow phenomena of two stacked fuel blocks and the modifiable gap is introduced between fuel blocks. Cross flow was evaluated from the difference between measured outlet flow and inlet flow. Using the experimental results, ANSYS CFX 13 which is commercial computational fluid dynamics code was validated to confirm the applicability of the CFD analysis on the cross flow phenomena. Furthermore, characteristics of cross flow is discussed in this paper.

CROSS FLOW EXPERIMENT FOR CORE OF PMR200

Experimental Facility and Conditions

In order to understand cross flow phenomena, cross flow experiment was designed and the full-scale two stacked fuel blocks experimental facility was constructed. Two types of gaps, wedge-shaped gap and parallel gap, were formed between two fuel elements. The schematic view of experimental apparatus was described in Figure 1. Air at ambient conditions was used as working fluid. The air flows through the test section from upstream block to downstream block. Inlet flow rate of upstream block, outlet flow rate of downstream block, pressure drops in coolant channels and pressure distribution in cross gap can be measured in this experimental facility. Cross flow rate can be evaluated from the difference between measured outlet flow rate and inlet flow rate. Test section was designed to be able to change the shape of the cross gap.

The ambient air is introduced to the test section from the top to the bottom and discharged through the blower, connected to the bottom of the test section. Figure 2 is the actual experimental apparatus. Two types of gaps, wedge-shaped gap and parallel gap were simulated and the sizes of the gaps were selected to be 0.5, 1, 2, 4 and 6 mm. Outlet flow rates were set to be 0.1 ~ 1.35 kg/s which are evaluated to be ranged between 4,000 and 54,000 in Reynolds numbers at coolant channel. 6-hole averaging pitot tubes were installed at inlet and outlet pipes to measure flow rates. From the difference between inlet flow rate and outlet flow rate, the cross flow rate was obtained.

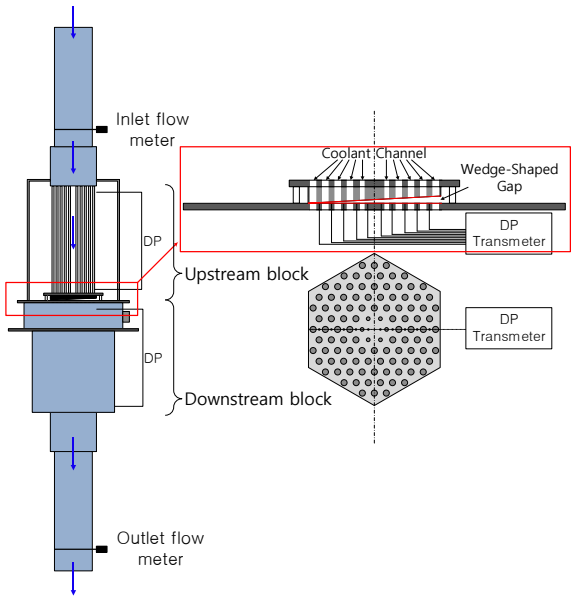

Figure 1 Schematic view of experimental apparatus

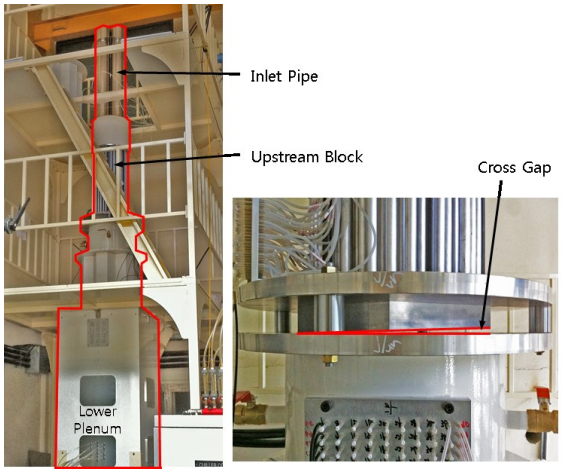

Figure 2 Experimental apparatus and cross gap

Experimental Results

Figure 3 and Figure 4 present the experimental results of the cross flow rate for whole cases. The absolute value of the cross flow rate increases with the main flow rate as seen in Figure 3-(a) and Figure 3-(b). In the cases of parallel gap, the cross flow rate is obviously higher than that in the wedge-shaped gap cases because the parallel cross gap has twice larger area than the wedge-shaped gap. In order to find out the characteristics of cross flow, the ratio of the cross flow rate was plotted as main flow rate as presented in Figure 3-(c) and Figure 3-(d). The ratio of the cross flow rate, CR, can be expressed as

$$CR = \frac{m_{cross}}{m_{main}}, \tag{1}$$

where m_{cross} is the mass flow rate of the cross flow and the m_{main} is the main flow rate which means the outlet mass flow rate of the downstream block. Even though the ratio of the cross flow rate is nearly constant for each gap size case, it decreases when the gap size is 6.0 mm, while it increases when the gap size is 0.5 mm. In order to identify the relation of the gap Re to the cross flow, the ratio of the cross flow was plotted as the gap Re in Figure 4. The gap Re number is defined as

$$\mathrm{Re}_{gap} = 4\frac{m_{cross}}{\mu P}, \tag{2}$$

where μ is the dynamic viscosity of the air and P is the wetted perimeter which is expressed as

$$P_{wedge} = 10a$$

$$P_{parallel} = 12a, \tag{3}$$

where a is the length of one edge of the hexagonal interface at the cross gap. In the cases of wedge-shaped gap, the air flows into 5 faces of the cross gap opening. On the other hand, in the parallel gap cases, the air flows into 6 faces of the cross gap opening.

Since the cross flow rate increases linearly with the main flow rate as shown in Figure 3, the ratio of the cross flow rate has almost constant value as plotted in Figure 4. It means the ratio of the cross flow is more affected by the size of the gap than by the gap Re number and, therefore, the shape and size of the gap are the important factors of the cross flow.

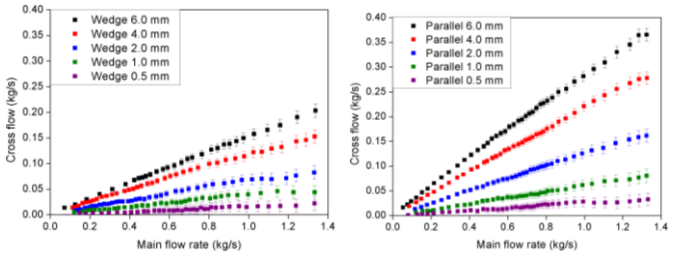

(a) Cross flow rate: Wedge (b) Cross flow rate: Parallel

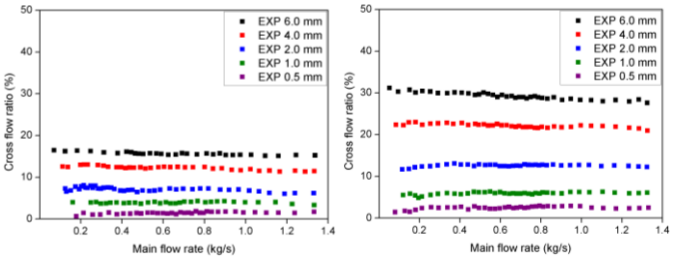

(c) Cross flow ratio: Wedge (b) Cross flow ratio: Parallel

Figure 3 The cross flow rate and the cross flow ratio to the main flow rate

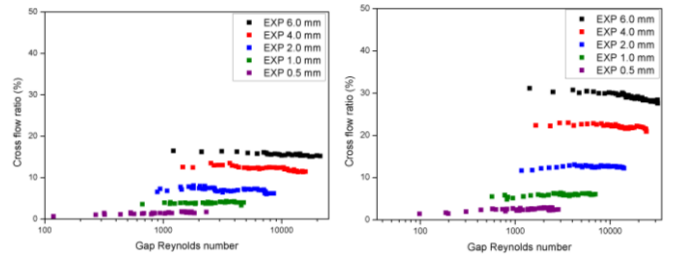

(a) Cross flow ratio: Wedge (b) Cross flow ratio: Parallel

Figure 4 The ratio of the cross flow rate to the gap Re number

Even though the ratio of the cross flow rate is nearly constant along the gap Re, the slope of the graph exhibits different trend depending on the size of the gap when it is magnified. In the case of 6 mm wedge-shaped gap, the ratio of the cross flow decreases as the gap Re number increases as shown in Figure 5. In this case, the range of the gap Re number is approximately 2000 ~ 21000 at 0.1 ~ 1.35 kg/s of the main flow rate as tabulated in Table 5, which means that the flow regime of this case is dominantly turbulent. In the case of 1.0 mm wedge-shaped gap, the ratio of the cross flow rate is almost constant (see Figure 6). The gap Re numbers are approximately 500, 3400, and 4600 at 0.1 kg/s, 0.8 kg/s, and 1.35 kg/s of the main flow rates, respectively. Therefore, it can be concluded that the flow regime changes from laminar to turbulent and as a result, the graph reveals the turnaround of the cross flow ratio. Figure 7 shows the ratio of the cross flow rate of 0.5 mm wedge-shaped gap. In this case, the ratio of the cross flow increases with the gap Re. The gap Re number in this case ranges from 350 to 2300 at main flow rate of 0.1 ~ 1.35 kg/s, which implies the flow regime in this case is dominantly laminar flow.

In the cases of parallel gap, a consistent tendency with the wedged gap cases was observed as indicated in Figure 8, Figure 9, and Figure 10 even though the trend of the cross flow ratio with 1 mm gap is less distinctive. From these results of the experiments, it was deduced that the tendency of the cross flow ratio to the gap Re is affected by the flow regime and the cross flow ratio increases with the gap Re if the gap Re number is smaller than 1000, and then maintains nearly constant value, after that decreases clearly when Re number is over 5000.

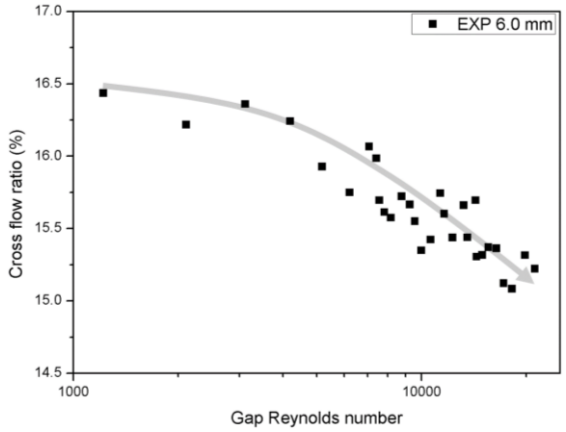

Figure 5 The ratio of the cross flow rate: 6 mm wedge-shaped gap

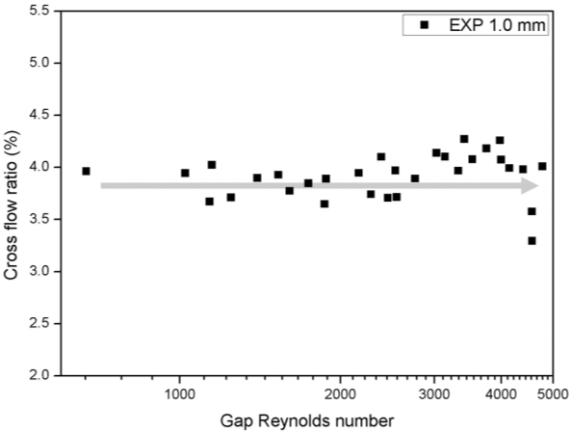

Figure 6 The ratio of the cross flow rate: 1 mm wedge-shaped gap

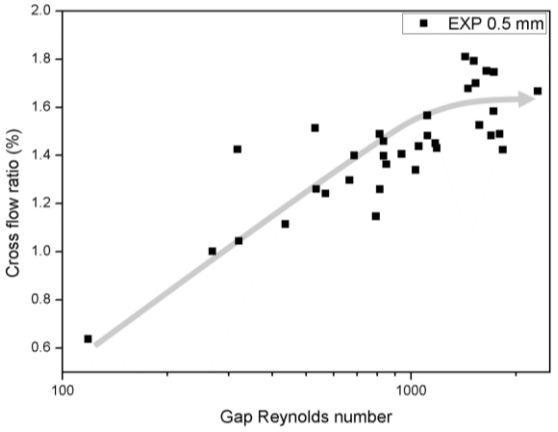

Figure 7 The ratio of the cross flow rate: 0.5 mm wedge-shaped gap

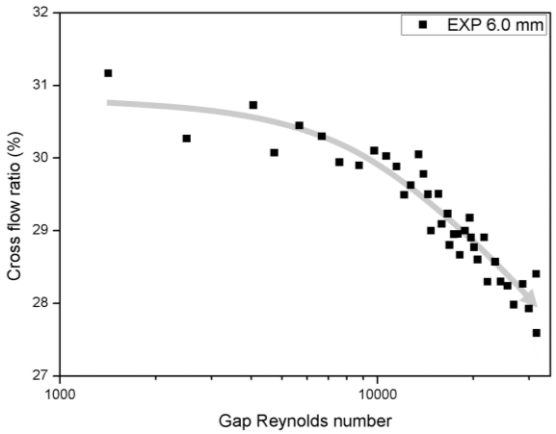

Figure 8 The ratio of the cross flow rate: 6 mm parallel gap

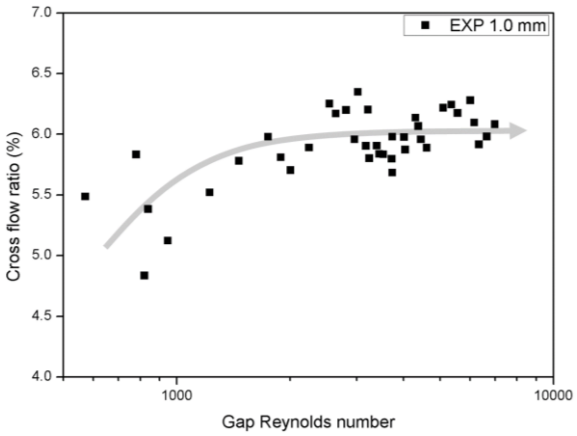

Figure 9 The ratio of the cross flow rate: 1 mm parallel gap

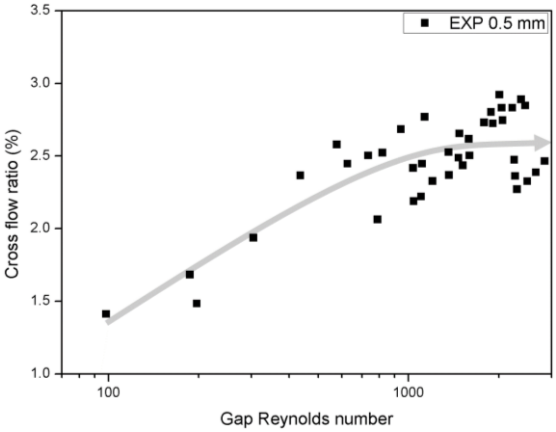

Figure 10 The ratio of the cross flow rate: 0.5 mm parallel gap

CFD ANALYSIS

From the experiments, the mass flow rate of the cross flow and the ratio of the cross flow were obtained. However, the form loss coefficient consists of the average pressure different between outside of the cross gap and inlet of the downstream block and the average velocity of the cross flow at the cross gap opening. And the averaged value of the inlet pressure at the entire holes could not be measured in the experiment because of the vena contracta. Therefore, in this study, the prediction capability of the CFD for this experiment was validated and the form loss coefficient of the cross flow was obtained with the CFD analysis results. In this section, the calculation conditions for the CFD analysis, validation results with the experimental data, and the form loss coefficient obtained from the CFD analysis were presented.

Numerical Models and Boundary Conditions

To apply the CFD code, the prediction capability of CFX 13 was validated by comparing the calculation results from the experimental data. This section introduces the computational domain, boundary conditions, applied mesh, and physical models of the CFD analysis and the calculation results will be presented in the next section in conjunction with the experimental data.

Figure 11 shows computational domain and mesh structure for the case of wedge-shaped gap with 6 mm width. In the present simulation, GAMBIT 2.2.30 was used for generating geometry and mesh grid. Approximately 9 million hexahedra mesh were used for the present simulation. Wall y+ value was approximately 20. The working fluid used was air at ambient temperature and pressure. Since the pressure drop through two fuel blocks is under 5000 Pa at maximum flow rate condition, the properties of fluid were assumed to be constant. The Shear Stress Transport (SST) model of Menter (1994) [9] with an automatic wall treatment based on the Reynolds Averaged Navier-Stokes (RANS) equation was adopted for turbulence modeling since the SST-k-ω model is able to produce good results for the flow with a separation. In addition, better results could be obtained by applying the transitional Gamma-Theta model [10]. The turbulence numeric and the advection fluxes were evaluated using a high resolution scheme that is second-order accurate and bounded in the current analyses. Residual for convergence criteria of iteration was set under 10-5. The calculation conditions were set according to experimental conditions. The computational domain consists of the opening boundary condition, outlet boundary condition and wall boundary condition. The opening boundary condition was imposed on the entrance of the upstream block and the cross gap between blocks. In the boundary details, the Mass and Momentum was set to be Opening Pres. and Dirn with a Relative Pressure of 0 Pa. The outlet of the downstream block was defined as the mass flow rate boundary condition. No slip wall and smooth wall were adopted as wall boundary conditions. Widths of the cross gaps were selected to be 0.5, 1, 2, 4, and 6 and outlet flow rates were varied from 0.1 to 1.35 kg/s as in the experiment.

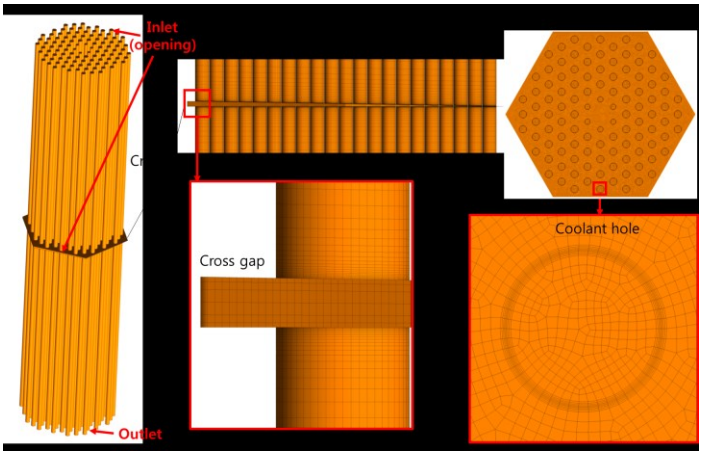

Figure 11 Computational domain and mesh structure

Grid Convergence Study

A grid convergence study is conducted using current grid (8.76 million cells) and coarser grid cases (3.98 million cells, 1.77 million cells and 0.81 million cells) with 1 kg/s outlet flow rate and 6 mm wedge-shaped gap. The meshes used in grid convergence study are presented in **Figure 12**. The mass flow rates at the cross gap and pressure drops from the inlet to the outlet were compared between the current and coarse mesh cases as plotted **Figure 13**. The extrapolate solution, ϕ, was obtained by using Richardson Extrapolation method [11, 12]. Since the errors of the Mesh 4 case are under 1%, it was selected for this analysis and the results indicate that the current grid is sufficiently fine for simulating the cross flow phenomena in the two-stacked fuel block.

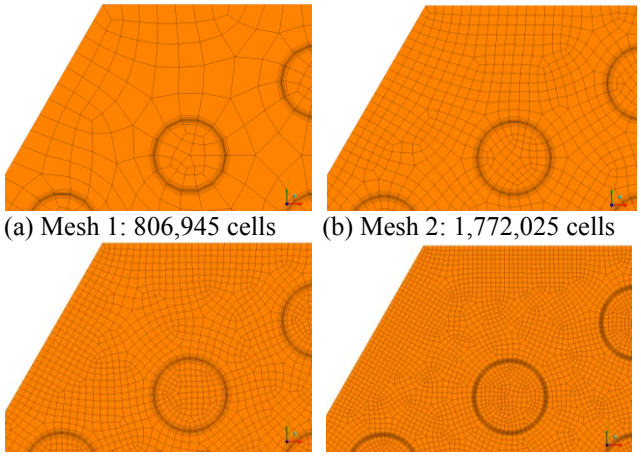

(a) Mesh 1: 806,945 cells (b) Mesh 2: 1,772,025 cells

(c) Mesh 1: 3,983,165 cells (d) Mesh 2: 8,761,490 cells

Figure 12 Finite element meshes used in grid convergence study

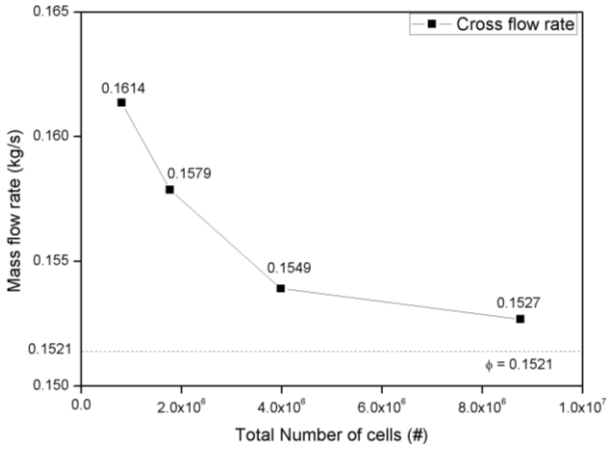

(a) Mass flow rate at the cross gap

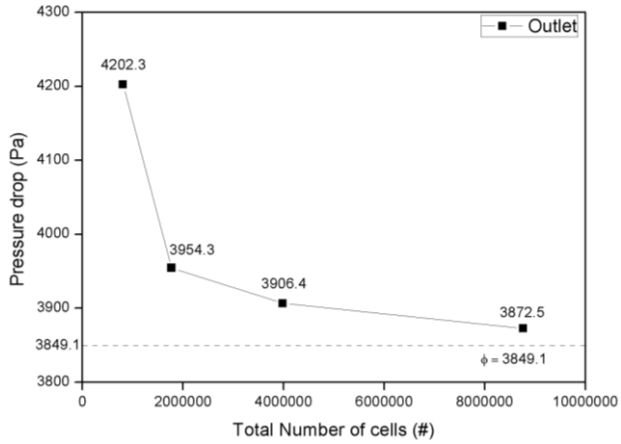

(b) Pressure drop from inlet to the outlet

Figure 13 Grid convergence test

Comparison Results between CFD Calculation and Experiment

In order to verify the prediction capability of the CFD code, the calculation results were compared with the experimental results in Figure 14 to Figure 16. In Figure 14 and Figure 15, the analysis results for the largest and smallest gaps are presented and the comparison results of whole cases are plotted in Figure 16. As seen in Figure 14 and Figure 15, the results of the CFD calculation showed fairly good agreement with the experimental data. Especially, the increasing trend of the cross flow ratio with the small gap size and the reverse trend with the large gap size were well captured by the simulation. This means that for the fully laminar or turbulent regions, the present CFD analysis reproduced the cross flow phenomena accurately. However, slight discrepancies were observed with the wedged gap when its size is in the range of 1~2 mm. In general, the CFD calculation under-predicted the experimental data slightly when the main flow rate is low and accordingly, the Reynold number is low. Nevertheless, the disagreement of the results between the experiment and the CFD calculation is within 2% in the absolute value of the cross flow ratio. Figure 17 presents the comparison between the experimental data and the CFD calculation results for whole cases. Considering uncertainty of

the experiment the discrepancies can be considered insignificant.

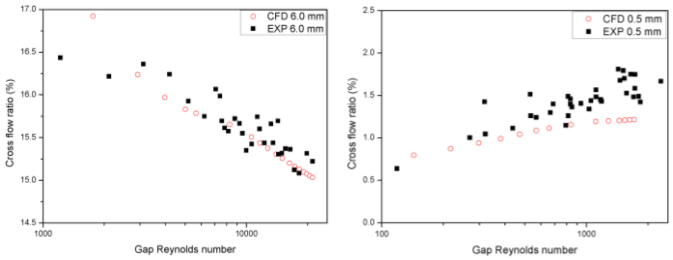

(a) Gap size 6 mm case (b) Gap size 0.5 mm case

Figure 14 Comparison results for the wedge-shaped gap cases

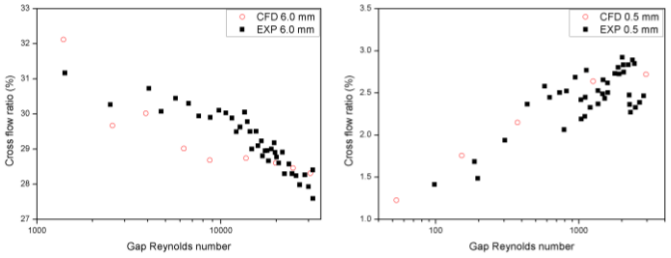

(a) Gap size 6 mm case (b) Gap size 0.5 mm case

Figure 15 Comparison results for the parallel gap cases

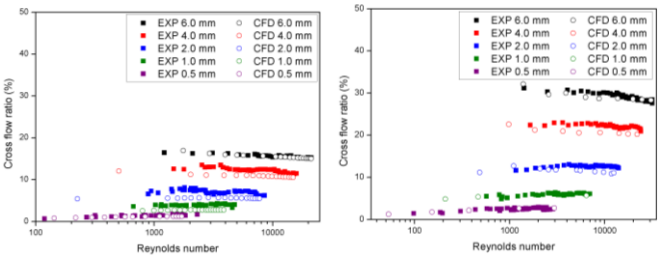

(a) Wedge-shaped gap (b) Parallel gap

Figure 16 Comparison results for whole cases

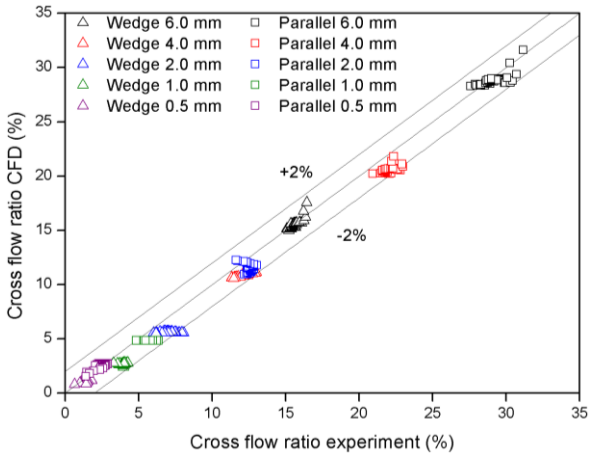

Figure 17 Comparison of the CFD prediction and experiments for whole cases.

Pressure Loss Coefficient

The pressure loss coefficient in the cross gap plays a crucial role when estimating the cross flow rate using a lumped parameter code, which is used frequently for the safety and performance analysis of a prismatic core of VHTR. Such a code determines the cross flow rate from the pressure difference between two fuel blocks and the pressure loss across the cross gap. In order to provide the loss coefficients for the lumped parameter codes, the variables from CFD analysis results were analyzed. The loss coefficient, K, is defined as

$$K = \frac{\Delta P}{\frac{1}{2}\rho v^2}, \quad (3)$$

where ΔP is the pressure drop between outside of the cross gap and the inlet of the downstream fuel block at the cross gap and v is the velocity of the cross flow at the cross gap opening. In order to obtain the loss coefficients for the cross gap, the pressures at entire coolant channels need to be averaged and the averaged value was obtained from the CFD calculation results. For consistency, velocity of the cross flow at the cross gap opening was also calculated with the CFD. The loss coefficients with the wedge-shaped gap and parallel gap are plotted in Figure 18 along the gap Re number. The pressure loss coefficient of the cross flow decreases as the gap Re number increases until 2000 and the loss coefficient becomes constant. The tendency of the variation of the cross flow ratio with the main flow rate can be interpreted by loss coefficient of cross flow with gap Re number. When the gap Re number is under 2000, since the loss coefficient decreases, the ratio of the cross flow increase as seen in the graphs of the gap size 0.5 mm cases (see Figure 7, Figure 10, Figure 14-(b) and Figure 15-(b)). And the trend of the loss coefficient shows similar trend with friction factor in rough pipes. From the friction factor of the Darcy-Weisbach equation, the friction factor is inversely proportional to gap Re number. For turbulent flow, the friction factor of rough pipes becomes constant, dependent only on the pipe roughness.

From this analysis, it can be concluded that the cross flow is governed by gap Re number and it implies the cross flow shows different behavior according to flow regime. This analysis results will be used in order to develop a correlation for the pressure loss coefficient, which is required for the prediction of the cross flow rate using a lumped parameter code.

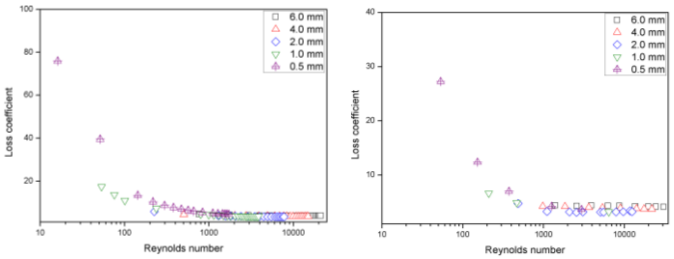

(a) Wedge-shaped gap (b) Parallel gap

Figure 18 Pressure loss coefficient at the cross gap

CONCLUSIONS

In the present paper, in order to understand the cross flow phenomena in the core of PMR200, a series of experiments were conducted. Two different types of cross gaps, wedge-

shaped gap and parallel gap, were used for the experiments and the cross flow rates were measured varying gap sizes and flow rates. In addition, CFD analysis was performed to validate its prediction capability and to investigate local phenomena. Conclusions can be summarized as follows:

- The results of the CFD analysis and experimental data are in good agreement even though CFD slightly underestimates in laminar-turbulent transitional region.
- The ratio of the cross flow is significantly affected by the cross gap size rather than the main flow rate.
- The cross flow ratio increases with the main flow rate if the gap Re number is smaller than 3000, but decreases otherwise. The flow pattern inside the cross gap is governed by the gap Re number.
- The pressure loss coefficient for the cross gap between the fuel blocks of PMR200 was obtained. The pressure loss coefficient of the cross flow decreases as the Re number increases until 2000 and becomes constant in high Re region.

Further study will be followed to develop the correlation of the cross flow loss coefficient, and then the correlation will be used to thermal-hydraulic analysis codes for the prismatic VHTR that incorporate lumped parameter model for a graphite block.

ACKNOWLEDGEMENT

This work was supported by a Basic Atomic Energy Research Institute (BAERI) grant funded by the Korean government Ministry of Education and Science Technology (MEST) (NRF-2010-0018759)

NOMENCLATURE

a	[m]	Length of one edge of the hexagonal interface at the cross gap
CR	[%]	Ratio of mass flow rate at the cross gap to outlet of the downstream block
K	[-]	Pressure loss coefficient
m	[kg/s]	Mass flow rate
P	[m]	Wetted perimeter
Re	[-]	Reynolds number
v	[m/s]	Velocity of air
Special characters		
ΔP	[Pa]	Pressure differnce
δ	[m]	Gap width
μ	[Pa·s]	Dynamic viscosity
ρ	[kg/m^3]	Density of air
ϕ	[-]	Extrapolated solution by Richardson Extrapolation method
Subscripts		
cross		Cross gap
main		Outlet of the downstream block
wedge		Wedge-shaped gap
parallel		Parallel gap
gap		Cross gap opening

REFERENCES

[1] Gauthier, J. C., Brinkmann, G., Copsey, B., Lecomte, M., 2006. ANTARES: The HTR/VHTR project at Framatome ANP. Nuclear Engineering and Design 236, 526-533

[2] Baxter, A., Rodriguez, C., Richards, M., Kuzminski, J., 2000. Helium-cooled Reactor Technologies for Accelerator Transmutation of Nuclear Waste. In: Proceedings of 6th Information Exchange Meeting on Actinide and Fission Product Partitioning and Transmutation, Madrid, Spain, December 11-13.

[3] Jo, C. K., Lim, H. S., Noh, J. M., 2008. Preconceptual Designs of the 200 MWth Prism and Pebble-bed Type VHTR Cores. In: Proceedings of International Conference on the Physics of Reactors. Interlaken, Switzerland, September 14-19.

[4] Idaho National Engineering and Environmental Laboratory, 2003. NGNP Preliminary Point Design – Results of the Initial Neutronics and Thermal-Hydraulic Assessment, INEEL/EXT-03-00870.

[5] Groehn, H. G., 1982. Estimate of Cross Flow in High Temperature Gas-cooled Reactor Fuel Blocks. Heat Transfer and Fluid Flow, Nuclear Technology 5, 392-400.

[6] Kaburaki, H., Takizuka, T., 1990. Crossflow Characteristics of HTGR Fuel Blocks. Nuclear Engineering and Design 120, 425-434.

[7] General Atomics, 1988. Graphite Design Handbook, DOE-HTGR-88111, Rev. 0.

[8] Lee, J. H., Yoon, S. J., Kim, E. S., Park, G. C., 2014. CFD Analysis and Assessment for Cross-flow Phenomena in VHTR Prismatic Core. Heat Transfer Engineering 35, 1151-1160.

[9] Menter, F. R., 1994. Two-equation Eddy-viscosity Turbulence Models for Engineering Applications, AIAA Journal 32, 1598-1605.

[10] Langtry, R. B., Menter, F. R., 2005. Transition Modeling for General CFD Applications in Aeronautics. AIAA Journal, In: Proceedings of 43rd AIAA Aerospace Sciences Meeting, Reno, NV, USA, January 10-13.

[11] Richardson, L. F., 1910. The Approximate Arithmetical Solution by Finite Differences of Physical Problems Involving Differential Equations, with an Application to the Stresses In a Masonry Dam, Philosophical Transactions of the Royal Society of London. Series A 210, 307-357.

[12] Richardson, L. F., Gaunt, J. A. 1927. The Deferred Approach to the Limit, Philosophical Transactions of the Royal Society of London. Series A 226, 299-361.